A Semiclassical coupled model for the transient simulation of semiconductor devices

Philippe Béchouche, Laurent Gosse

A SEMICLASSICAL COUPLED MODEL FOR THE TRANSIENT SIMULATION OF SEMICONDUCTOR DEVICES

PHILIPPE BECHOUCHE* AND LAURENT GOSSE†

Abstract. We consider the approximation of a microelectronic device corresponding to a $n^+ - n - n^+$ diode consisting in a channel flanked on both sides by two highly doped regions. This is modelled through a system of equations: ballistic for the channel and drift-diffusion elsewhere. The overall coupling stems from the Poisson equation for the self-consistent potential. We propose an original numerical method for its processing, being realizable, explicit in time and non-negativity preserving on the density. In particular, the boundary conditions at the junctions express the continuity of the current and don't destabilize the general scheme. At last, efficiency is shown by presenting results on test-cases of some practical interest.

Key words. Drift-diffusion equation, Schrödinger-Poisson equation, WKB ansatz, open quantum system, Robin boundary condition.

AMS subject classifications. 76W05, 65J10.

1. Introduction and modelling.

1.1. Preliminaries. The present paper scopes onto developing a fast, efficient and stable approach to 1D semiconductor components computations without directly processing any kind of kinetic equation; only moment-type approximations are to be used, in "high-field regime" though, in order to cope with "submicronic standards".

It is a well-known fact nowadays that a whole hierarchy of mathematical models ranges from quantum mechanics to transport equations eventually leading to "fluid-like" models, see *e.g.* [7, 33]. Two main tools exist for performing the first step, namely WKB and Wigner measures methods, see [2, 5, 30, 31]; the correct way to interpreting the WKB classical system being through a Vlasov equation, see [22, 26]. It is then at this "mesoscopic scale" that one introduces collisions between electrons and impurities (*i.e.* phonons, quantum representations of the crystal's vibrations) which thermalize the carriers population. This is rendered through a collision operator put on the right-hand side of the kinetic equation which is now meant to relax towards a local equilibrium called *Maxwellian* by analogy with Boltzmann's theory of rarefied gases, [14]. The passage from kinetic models to coarser ones always stems from prescribing a peculiar dependence of the kinetic density in its velocity variable; such simplifications can sometimes be justified by means of convenient time/space rescalings, consult [33] for a survey on these questions.

At this level, we take advantage of former results, mainly [13, 11, 3]; in these papers, coexistence of several qualitatively different areas has been clearly evidenced inside a standard n^+nn^+ diode, [10], under reasonable voltage biases. To each of these regions can be associated a particular rescaling of the kinetic transport model; roughly speaking, heavily doped zones (the *source* and the *drain*) exhibit "low-field" diffusive behaviour whereas inside the *channel* takes place "high-field" ballistic transport. To some extent, a schematic but acceptable picture goes as follows: carriers move inside the channel according to monokinetic solutions of the Vlasov-Poisson equation (because they accelerate, no shock is likely to appear at least at steady state) whereas

*Departamento de Matemática Aplicada, Universidad de Granada, Facultad de Ciencias, 18071 Granada (SPAIN). (phbe@ugr.es)

†Istituto per le Applicazioni del Calcolo (sezione di Bari), Via G. Amendola 122, 70126 Bari (ITALY) (l.gosse@ba.iac.cnr.it)..

they are "nearly Maxwellian" inside the source/drain regions where their position densities can be computed by means of a drift-diffusion approximation. We obviously expect to observe stabilization of transient dynamics leading to convergence onto some steady time-asymptotic regime (see *e.g.* [15, 34] for direct steady-state computations). We stress that our goal here is to devise a time-marching strategy.

Such a program clearly raises up an issue in terms of time-stepping compatibility, and this whatever the boundary conditions on each side of the channel. Indeed, any drift-diffusion equation, being of parabolic type, asks for a CFL restriction like $\Delta t = O(\Delta x^2)$ whereas ballistic regime is essentially of hyperbolic nature (signals travel at finite speed), thus requiring $\Delta t = O(\Delta x)$ instead. Of course, imposing the smallest value of Δt everywhere, despite ensuring stability, would result in an overwhelming smearing of the sharp profiles inside the channel. We thus selected a mixed implicit/explicit numerical strategy as described in §4.1. The channel being flanked on each side by low-field areas, deriving appropriate boundary conditions connecting these regions was necessary, so as oscillations won't develop. It has been observed that Dirichlet conditions aren't conclusive as they didn't allow for the scheme to relax toward a steady-state; however, imposing the current's continuity at the junctions leads to a nonlinear Robin boundary condition, [1, 17, 18, 19], for the drift-diffusion equations: it also remains stable and easy to implement, see §4.3. Obviously Dirichlet conditions are imposed on each side of the device and for the Poisson equation.

The remainder of the paper is devoted to numerical experiments as an outcome of the aforementioned general framework. A careful rescaling of a well-known GaAs device has been performed in §3 and practical results are displayed in §5. In particular, we observe stabilization in time toward a steady profile together with a satisfying residues decay. We also show the way current settles inside the device for large times; a reasonably constant current being the main goal in order to achieve reliable intensity/voltage diagrams (see especially Fig.5.6 in §5.5 where an original derivation leading to a real improvement of ballistic currents is proposed). Anyway, we aren't aware of any time-marching scheme able to stabilize onto steady-states with perfectly flat currents for such models. Presently, we found out Ohm's law, stipulating a linear dependence between currents and biases, being satisfied as soon as potential drops are strong enough. This was to be somehow expected as we developed the present approach for a high-field setting in which low biases don't really fit.

1.2. From quantum models to kinetic equations. We briefly recall the different levels for the modelling of charge carriers; the finest one here is nonrelativistic quantum mechanics. One considers thus a mixed-state, *i.e.* a statistical repartition of quantum states $\psi_\ell \in \mathbb{C}$ indexed by the (quantized) energy levels solution of the one-dimensional Schrödinger-Poisson equation in the parabolic band approximation: (m^* stands for the effective mass of the electron in the material under consideration)

$$i\hbar\partial_t\psi_\ell + \frac{\hbar^2}{2m^*}\partial_{xx}\psi_\ell = eU(t,x)\psi_\ell, \qquad \varepsilon_s\partial_{xx}U = e(\varrho - D). \tag{1.1}$$

The wave function $\psi_\ell(t,x)$ corresponds to an energy level E_ℓ of the homogeneous Hamiltonian, $\hbar$, e and m^* stand for Planck's constant, the charge and the effective mass of the electron in the considered material respectively. The Hartree equation renders a mean-field approximation of the Coulombian forces, with ε_0 being the dielectric permittivity of the medium. D is the given doping concentration and $\varrho(t,x)$

is electrons' density, which reads,

$$\varrho(t,x) = \sum_{\ell} F(E_\ell)|\psi_\ell(t,x)|^2,$$

with *e.g.* $F(E) = (1+\exp((E-E_F)/k_B\theta_0))^{-1}$ in case of Fermi-Dirac statistics, E_F being usually called the Fermi energy[1]. θ_0 is the ambient temperature, and k_B the Boltzmann's constant. The sum ranges therefore over the whole spectrum of the Hamiltonian consisting in an orthonormal basis of L^2; hence (1.1) is indeed a system of equations all coupled by the Poisson term U. With the next level of modelling comes into play the Wigner transform:

$$w(t,x,p) = \frac{1}{2\pi}\int_{\mathbb{R}} z\left(t, x+\frac{\hbar y}{2}, x-\frac{\hbar y}{2}\right)\exp(iyp).dy,$$

where

$$z(t,x,y) = \sum_{\ell} F(E_\ell)\psi_\ell(t,x)\overline{\psi_\ell(t,y)}.$$

One observes at once that:

$$\varrho(t,x) = \int_{\mathbb{R}} w(t,x,p).dp = z(t,x,x).$$

The Wigner transform solves the (pseudo-differential) Wigner equation,

$$\partial_t w + \frac{p}{\hbar m^*}\partial_x w - e\Theta[U]f = 0,\ \Theta[V] = \frac{i}{\hbar}\left\{U\left(t, x+\frac{\hbar}{2i}\partial_x\right) - U\left(t, x-\frac{\hbar}{2i}\partial_x\right)\right\},$$

completed by the Poisson equation as in (1.1). Passing to the (semi)classical limit $\hbar \to 0$, $w \rightharpoonup f(t,x,\xi) \geq 0$ in the sense of measures [31] and the pseudo-differential operator Θ becomes the standard Vlasov term $\partial_x U.\partial_\xi f$. It is usually at this intermediate level that electron-phonon collisions are introduced in the models (see however [2, 23]) by means of an integral operator on the right-hand side:

$$(1.2)\ \partial_t f + \xi\partial_x f + \frac{e}{m^*}\partial_x U\partial_\xi f = \mathcal{Q}(f), \qquad \varepsilon_s\partial_{xx}U = e(\varrho - D), \qquad E = -\partial_x U.$$

We shall not enter the details of $\mathcal{Q}(f)$ since different models exist like *e.g.* BGK or Fokker-Planck; however, they share the interesting property of admitting the same Maxwellian distribution, a fact that will be extensively used in the next section. At this level of description the electron and current density are the moments of f:

$$\varrho(t,x) = \int_{\mathbb{R}} f(t,x,\xi)d\xi, \qquad J(t,x) = \int_{\mathbb{R}} \xi f(t,x,\xi)d\xi.$$

2. Low and high field scalings inside a n^+nn^+ device. Our 1D problem combines two distinct zones according to the importance which is given to the phenomena rendered through $\mathcal{Q}$ in the equation (1.2); purely ballistic transport means $\mathcal{Q} \equiv 0$. However, we begin with the opposite case and mainly follow [11] in our presentation. Let us first recall some conventions: $L > 0$ stands for the characteristic

[1] it corresponds to an energy level for which the occupation probability is exactly one half.

device's length whereas $\varrho_0 \geq 0$ and $\theta_0 = k_B T/m^* \geq 0$, for an average value of the doping profile $D(x)$ and the lattice temperature. $U_{th} = k_B T/e$ is the thermal potential. Four (possibly) different velocity magnitudes appear: $v_{th} = \sqrt{\theta_0}$ is the **thermal velocity**. If τ_0 stands for an average value of the relaxation times[2] $\tau(x)$ inside the device, $v_{relax} = L/\tau_0$ is the **relaxation velocity**. Similarly, if $[\Phi]$ is the bias applied at the contacts, one defines the reference magnitude for the **drift velocity** as follows,

$$v_{drift} = \tau_0 \frac{e[\Phi]}{m^* L}, \tag{2.1}$$

whereas the **ballistic velocity** reads:

$$v_{bal} = \sqrt{\frac{2e[\Phi]}{m^*}}.$$

In a 1D framework, it is reasonable to render collisions by mean of a linear relaxation time operator thus we can start from the following kinetic equation to describe the dynamic of the electrons in the device.

$$\partial_t f + \xi \partial_x f - \frac{e}{m^*} E(t,x) \partial_\xi f = \frac{1}{\tau}\Big(\mathcal{M}(\theta_0)\varrho(x) - f\Big), \tag{2.2}$$

where the Maxwelian reads

$$\mathcal{M}(\theta_0) = \frac{1}{\sqrt{2\pi\theta_0}} \exp\left(-\frac{\xi^2}{2\theta_0}\right) \overset{\theta_0 \to 0}{\to} \delta,$$

where δ stands for the Dirac mass in zero; the electric field $E(t,x)$ is coupled to the Poisson equation by

$$\varepsilon_s \partial_{xx} U = e(\varrho(x) - D(x)), \qquad E(t,x) = -\partial_x U. \tag{2.3}$$

Remark 1. *Starting from here, we assume that junctions are rendered through sharp interfaces inside the device. Some quantities like e.g. the temperature will obviously be discontinuous across them. This modelling has already been widely used, see for instance [3, 8, 11, 12, 15].*

2.1. Drift-diffusion approximation. It is convenient to normalize the doping concentration and the potential bias: $D(x) = \varrho_0 \hat{D}(\hat{x})$ and $U(t,x) = [\Phi]\hat{U}(\hat{t},\hat{x})$ where we make use of rescaled variables defined as follows:

$$x = L\hat{x}, \qquad \xi = v_{th}\hat{\xi}, \qquad t = v_{drift}\frac{\hat{t}}{L}, \qquad \tau(x) = \tau_0 \hat{\tau}(\hat{x}).$$

Moreover the kinetic density rewrites:

$$f(t,x,\xi) = \frac{\varrho_0}{v_{th}} \hat{f}(\hat{t},\hat{x},\hat{\xi}).$$

The main assumption in this approximation is $v_{drift} \ll v_{th} \ll v_{relax}$; hence two small parameters naturally appear:

$$\epsilon = \frac{v_{th}}{v_{relax}}, \qquad \eta = \frac{v_{drift}}{v_{th}} \tag{2.4}$$

[2] for instance, in case $\mathcal{Q}$ is given by a BGK model.

which we suppose to be of the same order of magnitude. Then "low-field" is precisely meant to be the limit $\eta \simeq \epsilon \to 0$ thus (2.2) rewrites:

$$\epsilon\partial_t f + \xi\partial_x f - \frac{e}{m^*}E(t,x)\partial_\xi f = \frac{1}{\epsilon\tau}(\mathcal{M}(1)\varrho - f). \tag{2.5}$$

This regime describes the flow in highly doped areas (source and drain); (2.5) admits asymptotic expansions which allow to compute the two first moments of f in closed form. Since collisions are dominant, drift velocity is much smaller than thermal velocity and the mean free path can be considered infinitesimal, *i.e.* $o(1)$. Hilbert expansion leads to:

$$\partial_t\varrho + \partial_x J = 0, \qquad J = -d_n(x)\partial_x\varrho - \mu_n(x)E\varrho. \tag{2.6}$$

There, $\mu_n(x) = e\tau(x)/m^*$ is the electron mobility and $d_n(x) = \tau(x)\theta_0 = \mu_n U_{th} \geq 0$ appears to be a diffusion coefficient. In this regime, it is tacitly assumed that the solution of (2.5) is "nearly Maxwellian", *i.e.*

$$f(t,x,\xi) = \varrho(t,x)\mathcal{M}_{\theta_0}(\xi) + o(\epsilon).$$

2.2. Shur-Eastman/WKB ansatz for ballistic regime. This is somehow the opposite; we consider now the following variables:

$$x = L\hat{x}, \qquad \xi = v_{bal}\hat{\xi}, \qquad t = v_{bal}\frac{\hat{t}}{L}, \qquad \tau(x) = \tau_0\hat{\tau}(\hat{x}).$$

The kinetic density reads accordingly,

$$f(t,x,\xi) = \frac{\varrho_0}{v_{bal}}\hat{f}(\hat{t},\hat{x},\hat{\xi}).$$

The main assumption in this approximation is $v_{th} \ll v_{bal} \simeq v_{drift}$, which leads to the limit $\beta = v_{th}/v_{bal} \to 0$, while $\alpha = v_{drift}/v_{bal} = O(1)$. Thus comes out,

$$\partial_t f + \xi\partial_x f + \frac{e}{m^*}\partial_x U.\partial_\xi f = \frac{1}{2\alpha\tau}\mathcal{Q}(f), \qquad \theta_0 \to 0, \quad \partial_{xx}U = \gamma(\varrho - D). \tag{2.7}$$

Clearly, neither Hilbert nor Chapman-Enskog expansions are likely to lead to a diffusion-like equation. Instead, one obtains formally a Vlasov-Poisson system for which the kinetic density is of the *monokinetic* form at zero temperature (see [35] and [3], §5). This can be approximated by the so–called "WKB system", as in [25],

$$\partial_t\varrho + \partial_x\left(\frac{\partial_x\varphi}{m^*}\varrho\right) = 0, \qquad \partial_t\varphi + \frac{1}{2m^*}|\partial_x\varphi|^2 + eU = 0, \tag{2.8}$$

assuming that the wave functions behave like $\sqrt{\varrho}\exp(i\varphi/\hbar)$, or equivalently, that the solution of (2.7) reads $f(t,x,\xi) = \varrho(t,x)\delta(\xi - \partial_x\varphi(t,x))$, see [31]. Of course, $u = \frac{1}{m^*}\partial_x\varphi$ is meant to remain smooth[3] and this holds in particular for the accelerating particles $\partial_x u(t,x) \geq 0$ inside the channel. In §5 of [3], the authors suggest that the distribution f should be of the type $\delta(\xi - E\tau)$, which boils down to assuming that $u(t,x) \simeq \tau(x)E(t,x)$ at least after some time. This is indeed what we observe in the numerical results (in constrast with [11] where E and u look quite different at steady-state); see §5.4.

[3] if not, breakup occurs and multibranch solutions are to be sought instead, like in [22, 26, 29].

3. Rescaling the device. First of all let us remark that the device has not the same physical characteristics in the channel (ballistic zone) where there is a low doping concentration relatively to the source and the drain (Drift-diffusion zone). This implies that the electron mobility is higher in the channel as in the source and drain. The same occurs for the relaxation time in the same proportion. More precisely, let μ_1 be the mobility in the source and drain and μ_2 in the channel. We have

$$\frac{\mu_1}{\mu_2} = \frac{\tau_1}{\tau_2} = \frac{v_2}{v_1} \tag{3.1}$$

if we suppose that τ_1 (resp.τ_1) is proportional to L/v_1 (resp. to L/v_2). This means that if we want to see phenomena evolve at the same velocity, we have to scale the time in this proportion. An other way to explain this is if we scale the drift-diffusion equation first (with mobility μ_1) , then we have to scale the ballistic equation with the same scaling obtained in the drift-diffusion equation but with the mobility μ_2.

3.1. Rescaling the drift-diffusion equation. According to (2.6), the physical drift-diffusion model reads for $x \in [0, L]$, $t \geq 0$:

$$\varepsilon_s \partial_{xx} U = e(\varrho - D), \qquad \partial_t \varrho = \partial_x \left(\mu_1 U_{th} \partial_x \varrho - \mu_1 \varrho \partial_x U \right). \tag{3.2}$$

The first equation in (3.2) is Poisson's completed by a continuity equation. In the device's variables, the current density is given by: $J(t,x) = -d_1 \partial_x \varrho + \mu_1 \varrho \partial_x U$. The first part of the current is the diffusion term ($d_1 = \mu_1 U_{th}$) and the second part the drift term. The general way to process (3.2) starts by rescaling space and time variables according to the size of the device and some characteristic velocity which is to be chosen to convenience:

$$\hat{x} = \frac{x}{L}, \quad \hat{t} = \frac{t}{L/v_1}, \tag{3.3}$$

We can deduce an adimensionalized density ρ and a potential $\hat{U}$ as follows:

$$\varrho(t,x) = \varrho_0 \hat{\rho}(\hat{t}, \hat{x}) \qquad U(t,x) = U_0 \hat{U}(\hat{t}, \hat{x}). \tag{3.4}$$

The doping concentration is obviously treated accordingly:

$$D(x) = \varrho_0 \hat{D}(\hat{x}).$$

Here ϱ_0 stands for a mean density inside the device (obtained by *e.g.* doping concentration's arithmetic or geometric average) and U_0 is a reference value for the potential. We first rescale the Poisson equation so as to obtain,

$$\frac{\varepsilon_s U_0}{e \varrho_0 L^2} \frac{\partial^2 \hat{U}}{\partial \hat{x}^2} = \hat{\rho} - \hat{D}.$$

If we denote by $[\Phi_0]$ the applied bias, the scaled **Debye length** is given by

$$\gamma = \frac{\varepsilon_s [\Phi_0]}{e \varrho_0 L^2}.$$

At this level, we decide to choose $U_0 = \frac{e \varrho_0 L^2}{\varepsilon_s} = \gamma [\Phi_0]$ in order to scale the coefficient to 1. Thus the scaled Poisson equation rewrites:

$$\frac{\partial^2 \hat{U}}{\partial \hat{x}^2} = \hat{\rho} - \hat{D}. \tag{3.5}$$

Let us now rescale the continuity equation in (3.2); the outcome reads:

$$\frac{\partial \hat{\rho}}{\partial \hat{t}} = \frac{\partial}{\partial \hat{x}} \left(\frac{\mu_1 U_{th}}{v_1 L} \frac{\partial \hat{\rho}}{\partial \hat{x}} - \frac{\mu_1 U_0}{v_1 L} \hat{\rho} \frac{\partial \hat{U}}{\partial \hat{x}} \right). \tag{3.6}$$

A relevant quantity is the ratio between the diffusion and drift current: here it is U_{th}/U_0. We observe that in general, it is not possible to scale to unit simultaneously the scaled Debye length, the drift and diffusion terms. So in the present framework, we chose to scale to unit the scaled Debye length and the scaled drift term. Let us choose v_1 such that the drift velocity coefficient scales to 1 i.e. $\frac{\mu_1 U_0}{v_1 L} = 1$. In such a way (3.6) transforms into:

$$\frac{\partial \hat{\rho}}{\partial \hat{t}} = \frac{\partial}{\partial \hat{x}} \left(\frac{U_{th}}{U_0} \frac{\partial \hat{\rho}}{\partial \hat{x}} - \hat{\rho} \frac{\partial \hat{U}}{\partial \hat{x}} \right). \tag{3.7}$$

The scaled current density therefore reads

$$J(\hat{t}, \hat{x}) = -\frac{U_{th}}{U_0} \frac{\partial \hat{\rho}}{\partial \hat{x}} + \hat{\rho} \frac{\partial \hat{U}}{\partial \hat{x}}, \tag{3.8}$$

and (3.7)–(3.8) should be completed with the rescaled potential equation (3.5). A short computation with the numerical values given below shows that for high concentrations of doping, the drift term is more important than the diffusion term, for concentration of doping of $10^{19}/m^3$, both terms are of the same order of magnitude, and for concentration of doping lower, the diffusion term is dominant.

3.2. Rescaling the Ballistic equation. Let us now scale the equations (2.8) with the same scaling (3.3) in space and time but with v_2 instead of v_1 and (3.4) for the density and potential. Moreover we assume the phase scales in the following way

$$\varphi(t, x) = \varphi_0 \hat{\varphi}(\hat{t}, \hat{x}). \tag{3.9}$$

With this scaling equations (2.8) become

$$\begin{aligned} &\frac{\partial \hat{\rho}}{\partial \hat{t}} + \frac{\partial}{\partial \hat{x}} \left(\frac{\varphi_0}{m^* L v_2} \frac{\partial \hat{\varphi}}{\partial \hat{x}} \hat{\rho} \right) = 0 \\ &\frac{\partial}{\partial \hat{t}} \frac{\partial}{\partial \hat{x}} \left(\frac{\varphi_0 \hat{\varphi}}{m^* L v_2} \right) + \frac{1}{2} \frac{\partial}{\partial \hat{x}} \left(\frac{\varphi_0^2}{(m^*)^2 L^2 v_2^2} |\partial_{\hat{x}} \hat{\varphi}|^2 \right) + \frac{e U_0}{m^* v_2^2} \frac{\partial \hat{U}}{\partial \hat{x}} = 0. \end{aligned}$$

Note that we have derived w.r.t. $\hat{x}$ the second equation. In order to work with the same time scale as in the Drift-Diffusion case, we have to choose v_2 such that (3.1) is verified. Let let us set $u = \frac{\varphi_0}{m^* L v_2} \partial_{\hat{x}} \hat{\varphi}$. We can choose φ_0 such that $\frac{\varphi_0}{m^* L v_2} = 1$. We set for the scaled current $\hat{J} = \hat{\rho} u$. Then the scaled WKB equation (2.8) becomes:

$$\frac{\partial \hat{\rho}}{\partial \hat{t}} + \frac{\partial}{\partial \hat{x}} (\hat{\rho} u) = 0, \qquad \frac{\partial}{\partial \hat{t}} u + \frac{1}{2} \frac{\partial}{\partial \hat{x}} u^2 + \frac{e U_0}{m^* v_2^2} \frac{\partial \hat{U}}{\partial \hat{x}} = 0.$$

From now on, we shall always work with scaled quantities thus it makes sense to remove the "hats".

REMARK 2. **(Numerical values)** *Let us take the same test case as in [4, 11]: that is to say,* $m^* = 0.065 \times 9.109 \times 10^{-31} Kg$, $e = 1.602 \times 10^{-19} C$, $k_B = 1.38 \times$

$10^{-23}J/K$, $\varepsilon_s = 13.2\times 8.85418\times 10^{-12}F/m$, $T_0 = 300K$, $L = 0.8\times 10^{-6}m$. *Moreover in the classical zone, we take for the doping concentration* $D = 10^{24}/m^3$ *and for the electron mobility* $\mu_1 = \tau_1 e/m^* = 0.75$. *In the ballistic zone,* $D = 2\times 10^{21}/m^3$ *and* $\mu_2 = \tau_2 e/m^* = 4$. *These values imply that* $\varrho_0 = 5\times 10^{23}/m^3$, $U_0 = \frac{e\varrho_o L^2}{\varepsilon_s} = 438.6$. *Concerning the velocity* $v_1 = \frac{\mu_1 U_0}{L} = 4.111\times 10^8 m/s$ *which implies* $v_2 = v_1\mu_1/\mu_2 = 7.71\times 10^7 m/s$. *The scaled diffusion coefficient is* $d_1 = \frac{U_{th}}{U_0} = 5.9\times 10^{-5}$ *(and the scaled drift coefficient is* $\mu = 1$*). Finally we have* $eU_0/(m^* v_2^2) = 0.2$.

3.3. The kinetic equation. We finally rewrite the kinetic model (2.2); let us rescale the variables as follows:

$$x = L\hat{x}, \qquad \xi = v_{th}\hat{\xi}, \qquad t = v\frac{\hat{t}}{L}, \qquad \tau(x) = \tau_0\hat{\tau}(\hat{x})$$

where v is a velocity that is to be set according to the scaling which has been chosen. Moreover the adimensioned kinetic density rewrites:

$$f(t,x,\xi) = \frac{\varrho_0}{v_{th}}\hat{f}(\hat{t},\hat{x},\hat{\xi}).$$

As usual, we define an adimensioned density ρ and a potential Φ as follows:

$$\varrho(t,x) = \varrho_0\rho(\hat{t},\hat{x}) \qquad U(t,x) = \Phi_0\Phi(\hat{t},\hat{x}). \tag{3.10}$$

With this notation the adimensioned form of (2.2) reads:

$$\partial_{\hat{t}}\hat{f} + \Big(\frac{v_{th}}{v}\Big)\hat{\xi}\cdot\partial_{\hat{x}}\hat{f} - \left(\frac{U_0}{U_{th}}\frac{v_{th}}{v}\right)\partial_{\hat{x}}\Phi\cdot\partial_{\hat{\xi}}\hat{f} = \frac{v_{relax}}{v}\Big(\mathcal{M}(\theta_0)\hat{\varrho}(\hat{x}) - \hat{f}\Big). \tag{3.11}$$

Accroding to Remark 2, v can be chosen to be *e.g.* between $100v_{th}$ and $1000v_{th}$.

4. A staggered scheme for the coupled model. Hereafter we always consider working with the rescaled equations derived in the preceding section.

4.1. A semi-implicit discretization. We now aim at describing in full detail the numerical recipe we propose for the solving of the following adimensionalized problems:

$$(CL) \qquad \left\{\begin{array}{l} \partial_t\varrho + \partial_x J = 0, \\ J = -d\partial_x\varrho - \varrho\partial_x U, \ \varrho(t,x=0) = 1, \end{array}\right. \qquad x\in]0,x_L[;$$

$$(B) \qquad \left\{\begin{array}{l} \partial_t\varrho + \partial_x J = 0, \\ \partial_t u + u\partial_x u + \partial_x U = 0, \quad J = \varrho u, \end{array}\right. \qquad x\in]x_L,x_R[;$$

$$(CR) \qquad \left\{\begin{array}{l} \partial_t\varrho + \partial_x J = 0, \\ J = -d\partial_x\varrho - \varrho\partial_x U, \ \varrho(t,x=1) = 1, \end{array}\right. \qquad x\in]x_R,1[;$$

where all these PDE's are coupled through the Poisson equation:

$$(P) \qquad \left\{\begin{array}{l} -\partial_{xx}U = \varrho - D(x), \\ U(t,x=0) = 0, \quad U(t,x=1) = U_0 \le 0. \end{array}\right. \qquad x\in]0,1[.$$

We are given initial data $\varrho(t=0,.) = \varrho_0 \ge 0$, $D(x)\ge 0$ and $u(t=0,.)$ we usually take zero. We shall develop on the implementation of boundary conditions in $x = x_L, x_R$

rendering the junctions in §3.3. First, let us say that (CL), (CR) will be solved implicitly whereas (B) will be processed explicitly in time. Another important feature is that ϱ and u won't be known at the same abscissae (hence the use of "staggered"). The computational domain is the half-stripe $\mathbb{R}^+\times]0,1[$, which is parametrized by $\Delta x = \frac{1}{N} > 0$; we define,

$$x_j = j\Delta x = \frac{j}{N}; \qquad j = 0, ..., N.$$

We also define the following domains:

$$\begin{cases} \mathcal{B} = \{x_Q, x_{Q+1}, ..., 1 - x_Q\}, & x_Q = x_q + \frac{\Delta x}{2}, 1 - x_Q = x_{N-q} - \frac{\Delta x}{2}, \\ \mathcal{C}_L = \{x_0, x_2, ..., x_q\}, & \mathcal{C}_R = \{x_{N-q}, ..., x_N\}, \end{cases}$$

Thus $\vec{\varrho}_{n=0} = (\varrho_0(x_j))_{j=0,...,N} \in \mathbb{R}_+^{N+1}$. The boundary conditions read at the discrete level: $\varrho_{0,n} = \varrho(t_n, 0)$ and $\varrho_{N,n} = \varrho(t_n, x_N) = \varrho(t_n, 1)$.

4.2. Choosing the time-step Δt. We select a standard centered discretization for (CL), (CR); it reads: (n the time index, j the space one)

$$\begin{aligned} \varrho_{j,n+1} - \Delta t \tfrac{d(\varrho_{j+1,n+1} - \varrho_{j,n+1}) - d(\varrho_{j,n+1} - \varrho_{j-1,n+1})}{\Delta x^2} = \\ \varrho_{j,n} + \tfrac{\Delta t}{\Delta x}\Big(\Big\langle \mathbf{F}_{j+\frac{1}{2},n}, \mathbf{R}_{j+\frac{1}{2},n} \Big\rangle_{\mathbb{R}^2} - \Big\langle \mathbf{F}_{j-\frac{1}{2},n}, \mathbf{R}_{j-\frac{1}{2},n} \Big\rangle_{\mathbb{R}^2} \Big), \end{aligned} \tag{4.1}$$

where the following notations have been used:

$$\begin{aligned} \mathbf{F}_{j+\frac{1}{2},n} := \left\{ \max\left(0, \tfrac{U_{j+1,n} - U_{j,n}}{\Delta x}\right), \min\left(0, \tfrac{U_{j+1,n} - U_{j,n}}{\Delta x}\right) \right\}, \\ \mathbf{R}_{j+\frac{1}{2},n} := \left\{ \varrho_{j,n}, \varrho_{j+1,n} \right\}. \end{aligned}$$

Clearly, $<,>_{\mathbb{R}^2}$ stands for the standard $\mathbb{R}^2$ scalar product. At this stage, we tacitly assume that $\vec{\varrho}_n$ being known, we already have a way to produce the two borderline values $\varrho_{q+1,n+1}$ and $\varrho_{N-q-1,n+1}$. Thus, the scheme boils down to inverting a tri-diagonal $q \times q$ matrix reading:

$$\mathbf{M}_q = \begin{pmatrix} 1 + \frac{\alpha d\Delta t}{\Delta x^2} & -\frac{d\Delta t}{\Delta x^2} & 0 & \cdots & \\ -\frac{d\Delta t}{\Delta x^2} & 1 + \frac{2d\Delta t}{\Delta x^2} & -\frac{d\Delta t}{\Delta x^2} & 0 & \\ 0 & \ddots & \ddots & \ddots & \\ & & 0 & -\frac{d\Delta t}{\Delta x^2} & 1 + \frac{\beta d\Delta t}{\Delta x^2} \end{pmatrix},$$

where α, β can be 1 or 2 depending whether (4.1) is meant to approximate (CL) or (CR) because of the boundary conditions. Anyway, it is clearly unconditionally invertible since it is strictly diagonally dominant; thus the discretization (4.1) will remain stable as long as its right-hand side will be a convex combination, *i.e.* for a time step $\Delta t = O(\Delta x)$. In order to produce $\varrho_{q+1,n+1}$ and $\varrho_{N-q-1,n+1}$, we solve (B) by means of an explicit time-marching scheme already used in [24, 25], except that we set it up now together with a well-balanced strategy, as in [21] for the handling of the electric field. More precisely, from [24],

$$\varrho_{j,n+1} = \varrho_{j,n} - \frac{\Delta t}{\Delta x}\Big(\Big\langle \mathbf{A}_{j+\frac{1}{2},n}, \mathbf{R}_{j+\frac{1}{2},n} \Big\rangle_{\mathbb{R}^2} - \Big\langle \mathbf{A}_{j-\frac{1}{2},n}, \mathbf{R}_{j-\frac{1}{2},n} \Big\rangle_{\mathbb{R}^2} \Big), \tag{4.2}$$

with $j = q, ..., N - q - 1$ and,

$$\mathbf{A}_{j+\frac{1}{2},n} := \left\{ \max\left(0, u_{j+\frac{1}{2},n}\right), \min\left(0, u_{j+\frac{1}{2},n}\right) \right\}.$$

Now the velocity values $u_{j+\frac{1}{2},n}$ are sought on the staggered computational grid by means of a simple upwind well-balanced scheme:

$$u_{j+\frac{1}{2},n+1} = u_{j+\frac{1}{2},n} - \frac{\Delta t}{\Delta x}\Big(\mathcal{F}(u_{j+\frac{1}{2},n}, \tilde{u}_{j+\frac{3}{2},n}) - \mathcal{F}(\tilde{u}_{j-\frac{1}{2},n}, u_{j+\frac{1}{2},n})\Big). \tag{4.3}$$

$\mathcal{F}(u,v) = \frac{1}{2}(\max(u,0)^2 + \min(v,0)^2)$ is the standard upwind scheme and the modified values $\tilde{u}_{j-\frac{1}{2},n}$, $\tilde{u}_{j+\frac{3}{2},n}$ are computed according to the steady-state equation, $u\partial_x u + \partial_x U = 0$ out of resonance points, see Appendix A and [21] for details. We know from [21, 24, 25] that this approach for the solving of (B) will be stable for a time step $\Delta t = O(\Delta x)$.

Hence the algorithm proceeds as follows: knowing all $\vec{\varrho}_n$ and $u_{j+\frac{1}{2},n}$ ($j = q, ..., N-q-1$) at some time $t^n = n\Delta t$, we first update $u_{j+\frac{1}{2},n+1}$ inside $\mathcal{B}$ with (4.3) in order to deduce $\varrho_{j,n+1}$ by means of (4.2). Then, knowing $\varrho_{q+1,n+1}$ and $\varrho_{N-q-1,n+1}$, we can invert the implicit scheme (4.1) as soon as we have chosen a correct boundary condition to render the junction between the diffusive/ballistic zones.

4.3. A (nonlinear) Robin boundary condition. Let us mention first that junctions have been put at staggered abscissae, $x_{q+\frac{1}{2}}$, $x_{N-q-1-\frac{1}{2}}$, which correspond to the velocity unknowns. At these points, imposing Dirichlet boundary conditions leads to some kind of inconsistency because of a somewhat redundant definition of the current J between *e.g.* (CL) and (B). Numerically, it produced some spurious oscillations eventually leading to general instability. Moreover, in order to observe a constant current everywhere inside the device at steady state, it sounds reasonable to impose its **continuity** at the junctions between diffusive and ballistic areas. That is to say, at $x_{q+\frac{1}{2}}$,

$$u_{q+\frac{1}{2},n+1} = -d\frac{\varrho_{q+1,n+1} - \varrho_{q,n+1}}{\Delta x \varrho_{q+\frac{1}{2},n+1}} - \frac{U_{q+1,n+1} - U_{q,n+1}}{\Delta x},$$

which implies:

$$-d\frac{\varrho_{q+1,n+1} - \varrho_{q,n+1}}{\Delta x} = \varrho_{q+\frac{1}{2},n+1}\Big(u_{q+\frac{1}{2},n+1} + \frac{U_{q+1,n+1} - U_{q,n+1}}{\Delta x}\Big),$$

that we can approximate by means of

$$-d\frac{\varrho_{q+1,n+1} - \varrho_{q,n+1}}{\Delta x} = \big(\theta\varrho_{q+1,n+1} + (1-\theta)\varrho_{q,n+1}\big)\Big(u_{q+\frac{1}{2},n+1} + \frac{U_{q+1,n+1} - U_{q,n+1}}{\Delta x}\Big), \tag{4.4}$$

for $\theta \in [0,1]$. Hence one recognizes on the left-hand side of (4.4) the unknown flux which appears in (4.1) and the $\mathbf{M}_q$ matrix, and the right-hand side contains only values which can be deduced from the outcome of the explicit schemes used inside $\mathcal{B}$. Actually, only the average value $\varrho_{q+\frac{1}{2},n+1}$ has to be arbitrarily chosen as *e.g.* the arithmetic average $\frac{1}{2}(\varrho_{q+1,n+1} + \varrho_{q,n+1})$, $\varrho_{q,n+1}$ or $\varrho_{q+1,n+1}$, corresponding to $\theta = \frac{1}{2}$, $\theta = 0$ and $\theta = 1$ respectively.

REMARK 3. *This choice of boundary conditions corresponds to the solving of the following problem for the drift-diffusion equation (CL):*

$$\begin{cases} \partial_t \varrho + \partial_x J = 0, \qquad J = -d\partial_x \varrho - \varrho\partial_x U, \qquad x \in]0, x_L[, \\ \varrho(t, x = 0) = D(x = 0), \ -\partial_x \ln(\varrho)(t, x = x_L) = u + \partial_x U \end{cases}$$

where $u(t, x = x_L)$ is deduced from (B). This is a mixed (nonlinear) Robin-type boundary condition for a strictly parabolic equation. The well-posedness theory for problems

of this flavour is quite recent; it started with the paper by L. C. Evans [17] and then developed further into [1, 18, 19].

Of course, we presented everything in $x = x_{q+\frac{1}{2}}$, but the right junction $x = x_{N-q-1-\frac{1}{2}}$ is completely equivalent (with maybe a different choice of θ however).

4.4. Some stability results. First of all, we wish to state a result from [19] which we adapt to our situation involving only a uniformly elliptic linear operator:

THEOREM 4.1. *(Goldstein & Goldstein, [19]) Let $\beta_j(\xi)$ be a strictly increasing and continuous function. The problem:*

$$\begin{cases} \partial_t u = \partial_{xx} u, & x, t \in (0,1) \times \mathbb{R}^+, \\ (-1)^j \partial_x u(.,x) = \beta_j(u), & x = j \in \{0,1\}, \\ u(t=0,x) = f(x) \in L^1(0,1) & x \in (0,1), \end{cases}$$

has a unique mild solution u in $(0,1) \times [0,T]$ for any $T > 0$ given. Moreover, $u(t,.) \in L^\infty(0,1)$ and $\partial_t u(t,.) \in L^2(0,1)$.

Clearly in order to be complete, a full study of the coupled problem (even if neglecting the Poisson coupling equation) would be necessary before concluding to the stability of the whole model given by (CL)-(B)-(CR). However, the former theorem is a stepping stone in this direction. An interesting feature of our numerical approach (4.1)–(4.2) lies in a nonnegativity-preserving property for the density.

THEOREM 4.2. *Let $\theta = 0$ in (4.4), $\max_{j,n}(|u_{j+\frac{1}{2},n}| + |U_{j+1,n+1} - U_{j,n+1}|/\Delta x)\Delta t \leq \Delta x$ and $\vec{\varrho}_n \in (\mathbb{R}_+)^N$, then the whole scheme (4.1)–(4.2) preserves nonnegativity in the sense that $\vec{\varrho}_{n+1} \in (\mathbb{R}_+)^N$.*

Actually, we never used (4.1)–(4.2) with $\theta = 0$ because it looks like being the less accurate choice. However we were unable to prove Theorem 4.2 for $\theta > 0$.

Proof. The proof proceeds in 3 steps, namely the explicit part, then the implicit one and what happens at the junctions.

- We first observe that thanks to the prescribed CFL condition, the explicit parts of both schemes (4.1) and (4.2) turn out to be convex combinations of the values showing up on their right-hand sides. This has been precisely shown in previous paper, see *e.g.* Proposition 4.6 in [24] or §4.3 in [25].
- The implicit part of (4.1) is given by $\mathbf{M}_q$ which is a M-matrix in the terminology of [9], that is to say its entries satisfy:

$$m_{i,i} > 0, \qquad m_{i,j\neq i} \leq 0, \qquad |m_{i,i}| > \sum_{j\neq i} |m_{i,j}|.$$

So let's suppose we solve $\mathbf{M}_q \vec{x} = \vec{b}$ where $\vec{b}$ has nonnegative components, it is a classical fact that $\vec{x}$ will have only nonnegative components too. For completeness we recall its (quick) proof: let i_0 corresponds to the smallest component of $\vec{x}$, $x_{i_0} := \min(\vec{x})$. There holds:

$$m_{i_0,i_0} x_{i_0} = b_{i_0} - \sum_{j\neq i_0} m_{i_0,j} x_j \geq b_{i_0} - x_{i_0} \sum_{j\neq i_0} m_{i_0,j},$$

which implies:

$$x_{i_0} \geq \frac{b_{i_0}}{m_{i_0,i_0} + \sum_{j\neq i_0} m_{i_0,j}} \geq 0.$$

- It remains to observe that choosing $\theta = 0$ in (4.4) means that the boundary condition shows up only in the implicit part of (4.1). Let us focus on the left junction: inside $\mathbf{M}_q$, we have $\alpha = 2$ and $\beta = 1$. The condition (4.4) gives us another term which reads $u_{q+\frac{1}{2},n+1} + \frac{U_{q+1,n+1}-U_{q,n+1}}{\Delta x}$, but thanks to the CFL condition, we know that $\mathbf{M}_q$ remains diagonal-dominant even on this line. Hence the preceding computation garantees the nonnegativity-preserving property and we are done.

□

These computations are based on convexity arguments hence they somehow open the way to compactness for the whole scheme. However, we do not have any precise theory at the continuous level for (CL)-(B)-(CR) yet. This might constitute a direction for further investigation.

REMARK 4. *Actually the choice of the parameter θ is quite a delicate task when considering its importance in order to make the numerical scheme stabilize on a steady-state regime with flat currents (as can be seen on the numerical figures). Here is what we implemented in order to produce the numerical results of §5: first, we distinguished between the left junction where the solution is Lipschitz-continuous and the right one where it generally involves a discontinuity. Then we observed that it wasn't possible to code directly $\partial_x \ln(\varrho) = u + \partial_x U$ simply because it would require to apply the change of variable $v = \ln(\varrho)$ while solving the drift-diffusion equation, which isn't easy. Hence it becomes necessary to linearize the* $\ln(.)$ *function and this is where the $\theta \in [0,1]$ parameter comes into play through the mid-point rule. In case this linearization occurs in a smooth location, $\theta = \frac{1}{2}$ gives a second-order accuracy and is therefore sufficient. In case a discontinuity shows up, the upwind value is often the right choice, that is to say, the weight should go to the point from where the signal comes from (generally, it is the left side).*

5. Numerical validation with doping $5 \times 10^{22} m^{-3}$. In this section, we display some numerical results at steady-state for a standard GaAs device as already considered in [11, 3, 10, 35]. We took a discontinuous doping profile equal to 1 inside $x \in [0, 0.25[\cup]0.75, 1]$ and 0.002 elsewhere. We iterated the marching schemes presented in §3.2 until residues on $\vec{\varrho}_n$ decay lower than 10^{-15}. The resulting parameters are $d_1 = 0.00118$ and $eU_0/(m^* v_2^2) = 4$. We stress that neither "drift-diffusion nor mixed currents" are flat in the whole computational domain at steady-state; so in order to derive the current-voltage relations, we computed arithmetic averages of the results coming from both discretizations; we shall however propose a more interesting derivation in §5.5 relying on Well–Balanced ideas. 255 points have been used to sample the $[0,1]$ interval and the time-step is chosen adaptively in order to minimize the mixed scheme's numerical diffusion. The main difference between both curves in Fig.5.1 lies in slightly lower values for the drift-diffusion currents. Apart from that, both approaches appear to agree. However, we are about to see that despite the relations current-voltage may look similar, the densities and velocities are rather different.

REMARK 5. *It may sound reasonable to think about simulating directly the equation (2.2), at least to validate the outcome of our mixed scheme as in 1-D, the computational cost can be still considered reasonable. Indeed, performing the rescalings as in §3 leads to the following problem:*

$$v\partial_t f + v_{th}\xi\partial_x f + v_{th}\frac{U_0}{U_{th}}\partial_x U \partial_\xi f = v_{relax}(\mathcal{M}(\theta_0)\varrho - f),$$

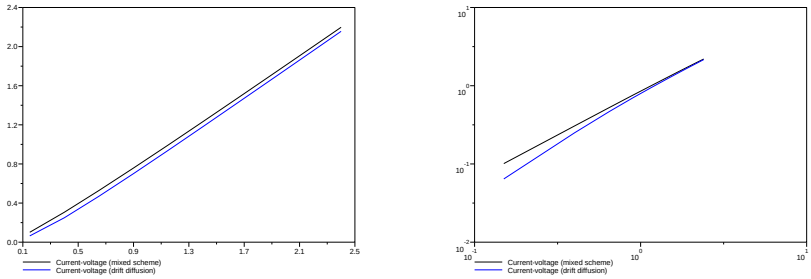

FIG. 5.1. *Current-Voltage relation with doping* $5 \times 10^{22} m^{-3}$ *(left, normal scale; right, log scale).*

supplemented by (3.5) and v *being a free parameter. Actually, it is also possible to evaluate all the parameters involved:* $\epsilon \simeq 0.09$, $\eta \simeq 0.3$ *(tending to zero in §3.1) and* $\beta \simeq 0.1$, $\alpha \simeq 2$ *(being* $o(1)$ *and* $O(1)$ *respectively in §3.2). However, there's at least one obstacle on this way: the problem still involves two different time scales, and two different Maxwellian distributions. Hence a direct upwind discretization of (3.11) is unstable because some boundary conditions are needed at each junction: a way out may consist in implementing numerically the formulas (16)–(17) in [8] (see also [16] for related questions). The schemes should also be asymptotic-preserving in the sense of [28, 27]. Finally, we notice from [12] that direct kinetic simulations deliver results quite similar to drift-diffusion ones.*

5.1. Weak bias: $[\Phi] = -0.2$**.** Essentially, the main difference between the mixed approach and the global drift-diffusion solving is that the last one always produces continuous solutions whereas jumps show up in the other ones. This is clearly demonstrated by the results in Fig. 5.2, even if the corresponding diffusion coefficient turns out to be relatively small. Velocities and densities turn out to be rather different for both approaches, especially when compared to the Poisson potential and the resulting electric field. We can observe that our prescribed boundary condition for the junction works fine for continuous solutions, but is unable to produce a flat current close to a shock. This can come from the fact it involves an average value, $\varrho_{q+\frac{1}{2},n+1}$ which should perhaps be derived more precisely. However, outside the junctions, currents look satisfying.

5.2. Moderate bias: $[\Phi] = -0.35$**.** In this case, the higher bias accelerates electrons; the outcome of both schemes is presented on Fig. 5.3. The residues decay is satisfying and the steady-state currents are reasonably flat. Densities and velocities are again very different for both approaches, quantitatively and qualitatively.

5.3. Higher bias: $[\Phi] = -0.5$**.** In this last case, the higher bias tends to flatten more the "mixed current", see Fig. 5.4 despite some sort of boundary layer on the right side. The potentials and the electric fields are quite similar for both approaches even if velocities and densities are still very different. Convergence in time is obtained in half the time it asked for with $[\Phi] = -0.2$.

5.4. Electric field and velocities inside the device. For completeness, we finally plot the fraction $u(x)/E(x)$ at steady-state since this quantity measures the conductivity as a function of the applied bias; see Fig. 5.5. We observe that independently of the bias, this fraction is practically constant in the zones where the

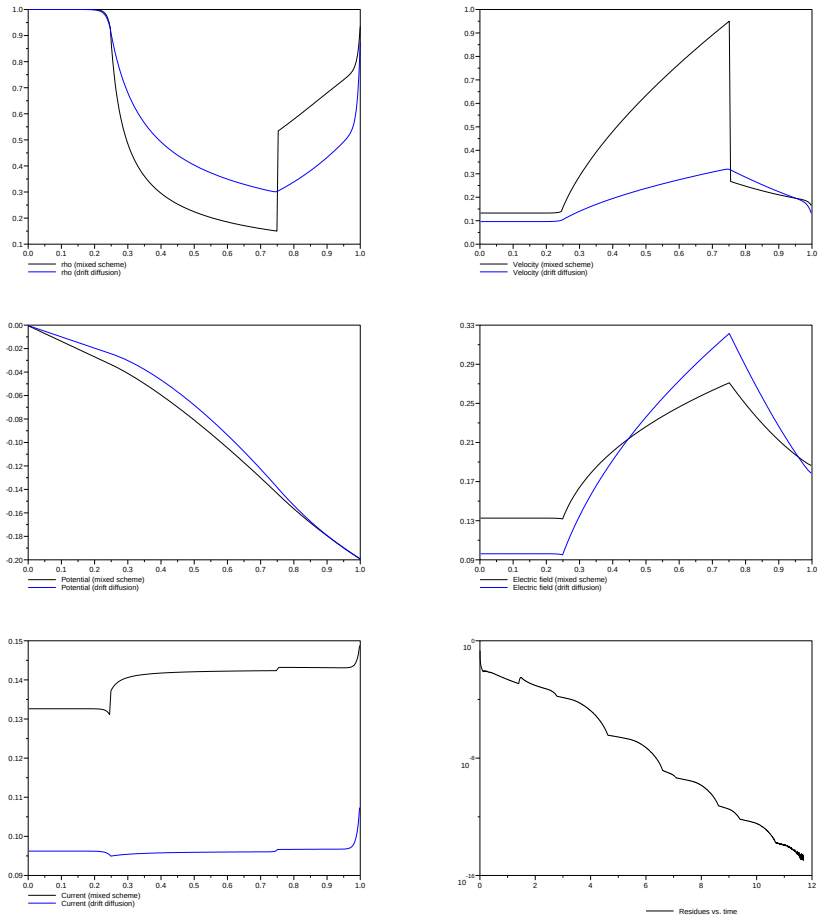

FIG. 5.2. *Carriers density, velocity, potential, electric field, currents and residues for an applied bias of* $[\Phi] = -0.2$. *(left to right, top to bottom).*

drift-diffusion algorithm is used (this reflects the smallness of the diffusion coefficient for high doping). However, it falls down strongly inside the channel even if increasing the bias improves things. Junctions are slightly visible, but the corresponding discontinuities don't seem to have strong effects on the global picture.

5.5. A different way to compute currents in the device. We finally propose a new way to compute steady-state currents inside the device, owing to the fact that a Well–Balanced discretization is used to solve the ballistic part (B) of the problem; see Appendix A for details. Actually, assuming (B) is stationary, one derives easily that the following equality holds:

$$J_{bal}(x) = \varrho(x)u(x) = \varrho(x)\sqrt{-2(U(x) - U(x_L)) + u(x_L)^2}. \tag{5.1}$$

The same way, one actually can compute stationary drift-diffusion like:

$$J_{DD} = -\varrho(d\partial_x \ln(\varrho) + \partial_x U). \tag{5.2}$$

On Fig.5.6, we compare the outcome of the very usual arithmetic averages with the

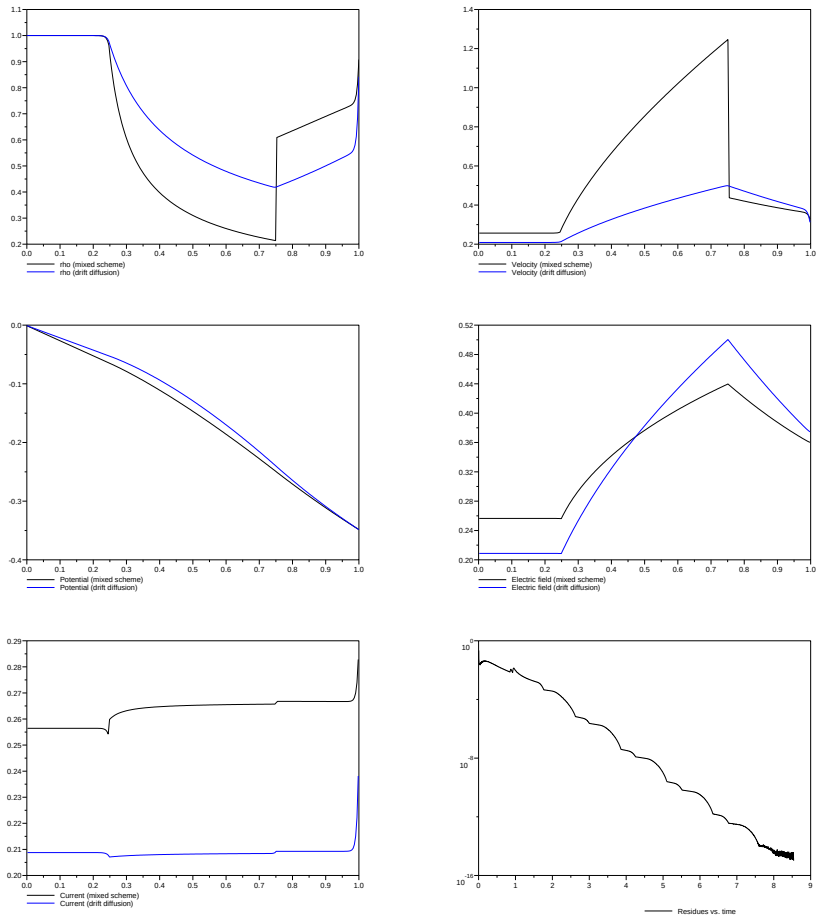

FIG. 5.3. *Carriers density, velocity, potential, electric field, current and residues for an applied bias of* $[\Phi] = -0.35$. *(left to right, top to bottom).*

formulas (5.1)–(5.2). One clearly sees the inside the ballistic channel, the resulting currents are *perfectly flat*, which has never been obtained before up to the authors' knowledge. Even the drift-diffusion currents are rendered in a slightly better way: for $[\Phi] = -0.35$, there's no jump around $x = x_R$. Nevertheless, this isn't meant to improve the treatment of the junctions where small discontinuities still appear. We believe that only a discretization of the type (6.1) can solve this issue.

6. Conclusion and outlook. We presented in this paper a first attempt to develop a robust mixed approach to transient semiconductor's computations relying on a simple time-marching strategy. The main obstruction to circumvent was the choice of a time-step which would ensure the compatibility of both the parabolic (drift-diffusion) and hyperbolic (ballistic) areas, left apart the derivation of a stable boundary condition at the junctions between the source/drain and the channel. For completeness, we display here the current-voltage relation for a doping value of $10^{24}m^{-3}$, see Fig.6.1. With a diffusion coefficient so low, both curves look very similar.

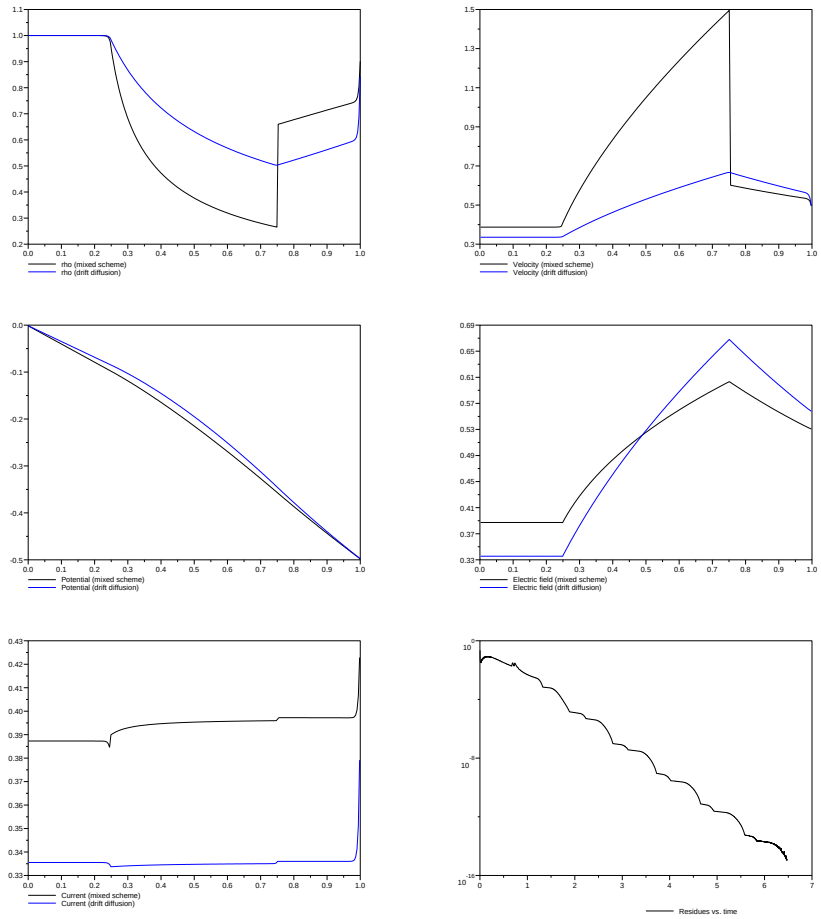

FIG. 5.4. *Carriers density, velocity, potential, electric field, current and residues for an applied bias of* $[\Phi] = -0.5$. *(left to right, top to bottom).*

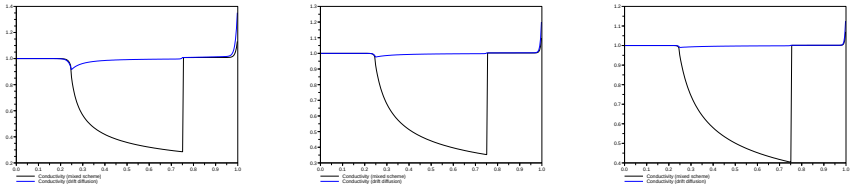

FIG. 5.5. *Steady state fraction* $u(x)/E(x)$ *for applied biases* $[\Phi] = -0.2, -0.35, -0.5$. *(left to right)*

There exist several ways of extending such an approach: one could be the inclusion of the energy bands, more accurate than the simple "effective mass" approximation made in (1.1). Indeed, such a simplification makes the whole model very close to the so–called "Drude theory of conduction" (see [2]), which is known to be quite crude. In order to improve the overall accuracy, an efficient algorithm to compute the Bloch decomposition in 1-D has already been studied in [26]. It may also be interesting

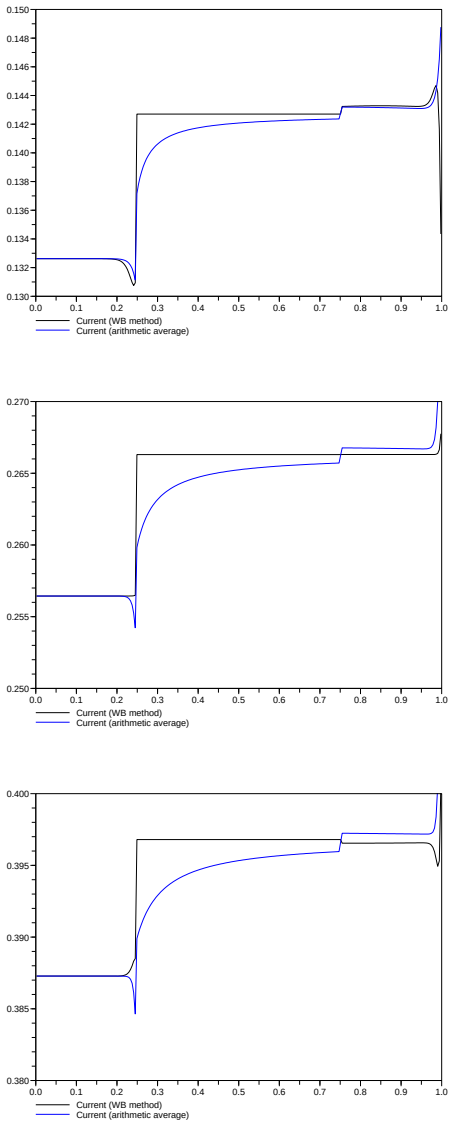

FIG. 5.6. *Steady state currents for the mixed scheme with* $[\Phi] = -0.2, -0.35, -0.5$. *(top to bottom)*

to use the sophisticate "multi-branch" routines of [22, 26] in this present context to achieve more precise simulations inside the ballistic channel. A routine able to handle phonons has been recently proposed in [23].

From the perspective of the "well-balanced" aspects of things, the big step would be to succeed in working with a good set of variables which would prevent from linearizing at the junctions (recall the delicate choice of the θ parameter, see Remarks 3 and 4). The first idea could be to replace the ϱ variable in (CL) and (CR) by

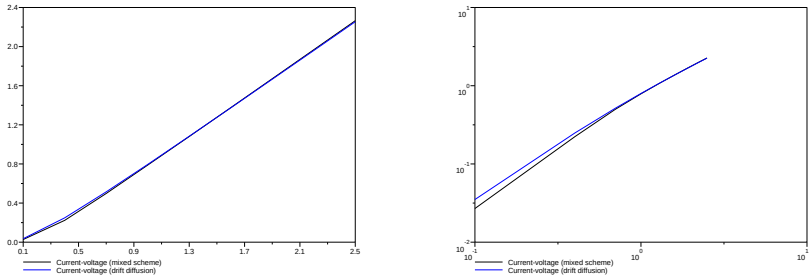

FIG. 6.1. *Current-Voltage relation with strong doping (left, normal scale; right, log scale).*

$z = \ln \varrho$. However, the price to pay is to make these drift diffusion problems nonlinear; indeed the equations become in the z variable

$$\left\{ \begin{array}{l} \partial_t z + d\big(\partial_{xx} z + |\partial_x z|^2\big) + \partial_{xx} U + \partial_x U \ \partial_x z = 0, \\ \exp(z)(\cdot, x = 0) = 1, \quad \partial_x z(\cdot, x = x_L) = u + \partial_x U, \end{array} \right. \tag{6.1}$$

the left junction being rendered through the last boundary condition. However, the nonlinear term is first-order, hence asks only for a mild CFL restriction.

Acknowledgments. The second author warmly greets the Mathematics Department of University of Granada for its hospitality (and Prof. J. Soler in particular). Both authors were partially supported by the EEC project HYKE (Hyperbolic and kinetic equations) #HPRN-CT-2002-00282.

Appendix A. Well-balanced for (B) in a nutshell.

In this short section, we follow [21] in order to explain quickly how to manage the forced Burgers equation appearing in (B) in such a way to approximate steady-states as best as possible. Let us suppose that $u(t,.) > 0$ holds (this is completely fair looking at the kind of steady regimes we have in mind to reproduce), we can rewrite the scalar balance law the following way:

$$\partial_t u + \partial_x \Big(\frac{u^2}{2} + U(t,x) \Big) = 0.$$

This clearly shows that steady states with $u \neq 0$ are given by the conservation law $\frac{u^2}{2} + U \equiv C^t \in \mathbb{R}$. At this point, it is easy to include the Poisson potential U in the upwind fluxes in order to maintain this property: thus we obtain the modified fluxes,

$$\mathcal{F}(u_l, u_r; U_l, U_r) = \frac{1}{2} \Big(\max(\tilde{u}_l, 0)^2 + \min(\tilde{u}_r, 0)^2 \Big),$$

with the upwinded values,

$$\tilde{u}_l = \sqrt{u_l^2 - 2(U_r - U_l)} \geq 0, \qquad \tilde{u}_r = -\sqrt{u_r^2 + 2(U_r - U_l)} \leq 0.$$

REFERENCES

[1] J. ARRIETA, A. CARVALHO, *Parabolic problems with nonlinear boundary conditions and critical nonlinearities*, J. Diff. Equations **156** (1999) 376–406.

[2] N.W. Ashcroft and N.D. Mermin, Solid-state physics, Holt; Rinehart and Winston 1976.
[3] A. Arnold, J.A. Carrillo, I. Gamba, C.W. Shu, *Low and high field scaling limits for the Vlasov and Wigner-Poisson-Fokker-Planck systems*, Transp. Theo. Stat. Phys. **30** (2001) 121–153.
[4] H.U. Baranger, J.W. Wilkins, *Ballistic structure in the electron distribution function of small semiconducting devices: general features and specific trends*, Phys. Review B **36** (1987) 1487–1502.
[5] P. Bechouche, N. Mauser, F. Poupaud, *Semiclassical limit for the Schrödinger-Poisson equation in a crystal*, Comm. Pure Applied Math. **54** (2001) 851–890.
[6] N. Ben Abdallah, P. Degond, *The Child-Langmuir law for the Boltzmann equation of semiconductors*, SIAM J. Math. Anal. **26** (1996) 364–398.
[7] N. Ben Abdallah, P. Degond, *On a hierarchy of macroscopic models for semi-conductors*, J. Math. Phys. **37** (1996) 3306–3333.
[8] N. Benabdallah, P. Degond, I. Gamba, *Coupling one-dimensional time-dependent classical and quantum transport models*, J. Math. Phys. (2002) **43** (2002) 1–24.
[9] A. Berman, R. Plemmons, Nonnegative matrices in the mathematical sciences, Academic Press (1979).
[10] K. Blotekjaer, *Transport equations for electrons in two-valley semiconductors*, IEEE Trans. Elec. Dev. **17** (1970) 38–47.
[11] J.A. Carrillo, I. Gamba, C.W. Shu, *Computational macroscopic approximations to the 1-D relaxation time kinetic system for semiconductors*, Physica D **146** (2000), 289–306.
[12] C. Cercignani, I. Gamba, G.W. Jerome, C.W. Shu, *Device benchmark comparisons via kinetic, hydrodynamic and high-field models*, Comput. Methods Appl. Mech. Engrg. **181** (2000), 381–392.
[13] C. Cercignani, I. Gamba, C.D. Levermore, *A drift-collision balance for a Boltzmann-Poisson system in boundad domains*, SIAM J. Appl. Math. **64** (2001), 1932–1958.
[14] P. Degond, *Mathematical modelling of microelectronics semiconductor devices*, in Some current topics on nonlinear conservation laws, L. Zhiao and Z. Xin Editors, Studies in Advanced Mathematics, AMS (2000).
[15] P. Degond, A. El Ayyadi, *A coupled Schrödinger Drift-Diffusion model for quantum semiconductor device simulations*, J. Comp. Phys. 191 (2002) 222–259.
[16] P. Degond, S. Jin, L. Mieussens, *A smooth transition model between kinetic and hydrodynamic equations*, preprint (2004).
[17] L. C. Evans, *Regularity properties for the heat equation subject to nonlinear boundary constraints*, Nonlinear Anal. 1 (1977) 593–602.
[18] A. Favini, G. Goldstein, J. Goldstein, S. Romanelli, *Nonlinear boundary conditions for nonlinear second order operators on C[0,1]*, Arch. Math. 76 (2001) 391–400.
[19] G. Goldstein, J. Goldstein, *Smoothing for nonlinear parabolic equations with nonlinear boundary conditions*, J. Math. Anal. Appl. 213 (1997) 422–443.
[20] F. Golse, F. Poupaud, *Limite fluide des équations de Boltzmann des semiconducteurs pour une statistique de Fermi-Dirac*, Asympt. Anal. 6 (1992) 135–160.
[21] L. Gosse, *A well-balanced flux splitting scheme designed for hyperbolic systems of conservation laws with source terms*, Comp. Math. Applic. **39** (2000) 135–159.
[22] L. Gosse, *Using K-branch entropy solutions for multivalued geometric optics computations*, J. Comp. Phys. **180** (2002) 155–182.
[23] L. Gosse, *Multiphase semiclassical approximation of the one-dimensional harmonic crystal. I. The periodic case*, J. Phys. A. Math. Gen. **39** (2006) 10509–10521.
[24] L. Gosse, F. James, *Numerical approximation of linear one-dimensional conservation equations with discontinuous coefficients*, Math. Comp. **69** (2000), pp. 987-1015.
[25] L. Gosse, F. James, *Convergence results for an inhomogeneous system arising in various high frequency approximations*, Numer. Math. **90** (2002), 721 – 753
[26] L. Gosse, P.A. Markowich, *Multiphase semiclassical approximation of an electron in a one-dimensional crystalline lattice – I. Homogeneous problems.*, J. Comp. Phys. **197** (2004) 387–417.
[27] L. Gosse, G. Toscani, *Space localization and well-balanced schemes for discrete kinetic models in diffusive regimes*, SIAM J. Numer. Anal. **41** (2003) 641–658.
[28] S. Jin, *Efficient asymptotic-preserving (AP) schemes for some multiscale kinetic equations*, SIAM J. Sci. Comput. **21** (1999), 441–454.
[29] Shi Jin, X.T. Li, J.G. Wohlbier, J.H. Booske *An Eulerian method for computing multivalued solutions of the Euler-Poisson equations and applications to wave breaking in klystrons*, Phys Rev E 70, 016502, 2004.
[30] J.B. Keller, *Semiclassical mechanics*, SIAM Review **27** (1985), 485–504.

[31] P.L. Lions and T. Paul, *Sur les mesures de Wigner*, Revista Mat. Iberoamericana **9** (1993) 553-618.
[32] P. Markowich, C.A. Ringhofer, C. Schmeiser, Semiconductor equations, Springer NY (1990).
[33] F. Poupaud, *Mathematical theory of kinetic equations for transport modelling in semiconductors*, in "Advances in Kinetic Theory & Computing", Series in Applied Math. **22** B. Perthame Ed. World Scientific (1994) 141–168.
[34] C. Ringhofer, *Computational methods for semiclassical and quantum transport in semiconductor devices*, Acta Numer. **3** (1997) 485–521.
[35] M.S. Shur, L.F. Eastman *Near ballistic transport in GaAs devices at 77K*, Solid. State Electr. **24** (1991) 11–18.